
Research Paper

Introduction of the Electrical Next Generation Impactor (eNGI) and Investigation of its Capabilities for the Study of Pressurized Metered Dose Inhalers

Susan Hoe,¹ Paul M. Young,^{1,2} Hak-Kim Chan,¹ and Daniela Traini¹

Received July 16, 2008; accepted October 15, 2008; published online October 31, 2008

Purpose. To introduce the design of the electrical Next Generation Impactor (eNGI), and validate its proposed function as a method of electrostatic characterization for pressurized metered dose inhaler (pMDI) formulations.

Methods. Flixotide[®] (fluticasone propionate), Ventolin[®] (salbutamol sulphate), and QVAR[®] (beclomethasone dipropionate) were used as model pMDIs in this study. At an airflow rate of 30 l/min, five individual actuations of each pMDI were introduced into the electrical low-pressure impactor (ELPI), Next Generation Impactor (NGI), and the eNGI. Charge profiles for each actuation were measured by the ELPI and eNGI, while mass profiles were recorded by the all three impactors.

Results. The difference in estimated mass median aerodynamic diameters and geometric standard deviations for all pMDIs using the NGI and eNGI were not found to be statistically significant ($p < 0.05$). The mean charge profiles from the ELPI and eNGI overlap well between 0.54 and 6.61 μm (Flixotide[®] and Ventolin[®]), and between 0.615 and 11.72 μm (QVAR[®]), where the majority of the impacted doses were collected. Conclusion: For the analysis of pMDIs, the eNGI is comparable to the NGI in measuring particle size distribution, while still being comparable to the ELPI in measuring charge distribution.

KEY WORDS: electrical next generation impactor (eNGI); electrostatics; ELPI.

INTRODUCTION

The deposition of particles in the respiratory tract has been commonly attributed to five mechanisms—inertial impaction, sedimentation, electrostatic forces, interception and diffusion. Electrostatic forces include space charge and image charge, of which space charge forces are only significant with dense aerosols. In general, after inhalation of an aerosol, charged particles approach the inner surface of the respiratory tract, induce a surface charge distribution of opposite polarity, and the subsequent attractive force, which deposits the particle on the surface, is termed image charge force (1,2). There have been a limited number of studies carried out with human volunteers exploring the distribution of deposited charged particles in the lung (3,4). Other experiments have instead used mathematical modelling and *in vitro* methods to predict the effect of specific charge on regional deposition (5–7).

Aerosol Charge Measurement

Devices used to measure aerosol charge are required to be Faraday wells or cages. A Faraday well consists of an inner

layer of conducting material, which conducts the charge carried by particles upon contact between the two surfaces. The outer layer is conductive and earthed, with the purpose of protecting the inner layer from environmental interference. The two layers are electrically isolated from one another. This becomes crucial for charge measurements as it ensures the current received from the inner layer is the sole result of the charge within the Faraday well. The *aerosol electrometer* is the simplest example of an aerosol charge measurement device, basically connecting an electrometer to a Faraday well via a probe which makes contact with the inner housing. In order to provide air flow for dispersion of a sample into the Faraday well, a vacuum pump is attached, as well as a filter for collection of the dispersed powder mass (from dry powder inhaler (DPI) actuations or pressurized metered dose inhaler (pMDI) actuations after propellant evaporation) (17,18). The design of the aerosol electrometer only measures net charge carried by an aerosol cloud, and cannot detect the nature of any possible bipolar charging within the cloud. As a result, it is unable to assess the relationship between particle size and charge (13,19).

The logical solution to this problem is to combine an impactor with an electrometer. The electrical low-pressure impactor (ELPI) is the most recent equipment to be used as an aerosol charge measurement device, based on the Berner multi-jet low pressure impactor (BLPI). It may be conceptualized as a vertical arrangement of 13 Faraday wells, with each well containing an impaction stage electrically isolated

¹Advanced Drug Delivery Group, Faculty of Pharmacy (A15), University of Sydney, Sydney, New South Wales 2006, Australia.

²To whom correspondence should be addressed. (e-mail: py@pharm.usyd.edu.au)

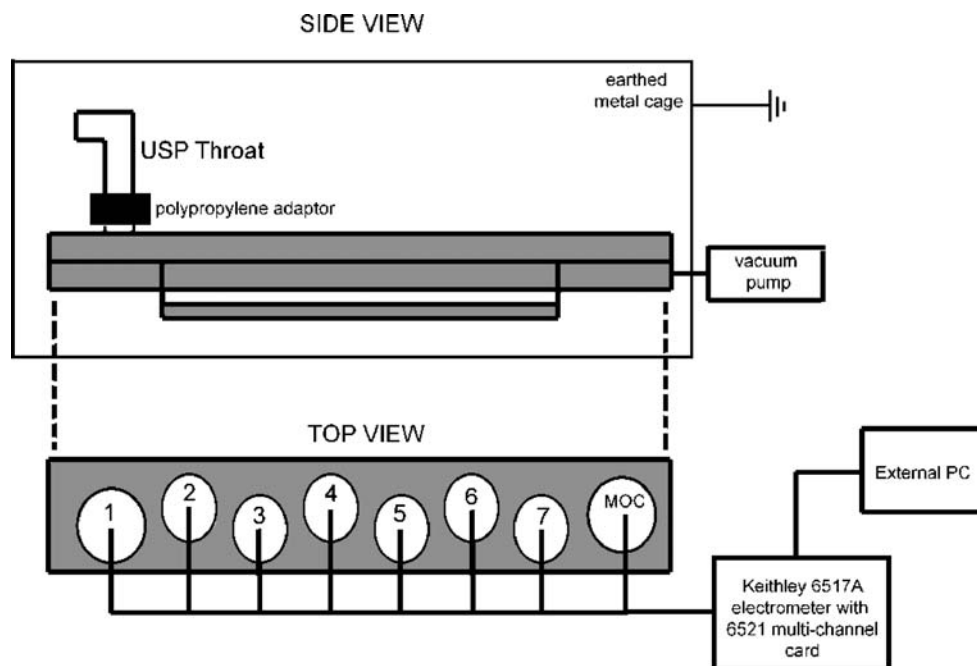


Fig. 1. Schematic diagram of the novel eNGI setup.

from the other stages. Stages 1 to 12 are each connected to a multi-channel femtoamp electrometer for real-time parallel current measurements (20). Each ELPI impaction stage contains a jet nozzle and impactor plate, designed with aerodynamic considerations to collect particles above a particular size (the *aerodynamic cut-off diameter*). A sample dispersed into the ELPI under vacuum air flow is separated into fractions of progressively smaller particle size from stage 13 (top stage) to stage 1 (bottom stage). As a whole, the ELPI measures particles in the size range from 30 nm to above 10 μm , when operated at its intended air flow rate of 30 l/min (14,21,22). In its original design, the ELPI possesses a corona charger which charges the dispersed aerosol. The current measured from each stage is converted into a calculation of average particle size, with the collective probe measurements compiled to determine particle size distribution. However, the corona charger may be turned off, such that the subsequent measurement of aerosol charge would be a reflection of triboelectrification (13, 14). A current vs. time profile for each stage is recorded by the ELPI VI 4.0 software, from which the total charge in each stage is calculated by integration of the area under the curve. Thus the ELPI is capable of measuring charge distribution corresponding with particle size.

Recent times have seen an increased interest in the electrostatic characterisation of pharmaceutical aerosols, particularly the relationship between charge and particle deposition. However, methods specifically dedicated to measurements of electrostatic charge in pharmaceutical aerosol formulations do not exist. The current standard for analysing the relationship between net charge and particle size is the ELPI, which was in fact originally designed for industrial and environmental aerosols, and is not a pharmacopoeia method. Another issue with the ELPI is that it is specifically designed to operate at 30 l/min, which enables the impactor to achieve a low pressure of 0.1 mbar within the stages (13–15). In

general, pharmaceutical impactors are designed to study lung deposition at a variety of flow rates.

Unlike the ELPI, the Next Generation Impactor (NGI) was specifically designed for measuring aerodynamic particle size distribution (PSD) of pharmaceutical aerosols, and has been included in the British Pharmacopoeia (BP) as a test method for this purpose. It is reasonable to expect that any potential design for an apparatus which simultaneously measures PSD and charge distribution would contain a pharmacopoeia-approved impactor. This article proposes the design of the electrical next generation impactor (eNGI), dedicated to the electrostatic characterization of pMDI formulations. In addition, the aim of this study was to validate this design against methods currently used for particle sizing (NGI) and electrostatic characterization (ELPI) of pharmaceutical aerosol formulations, using commercial pMDI formulations for analysis.

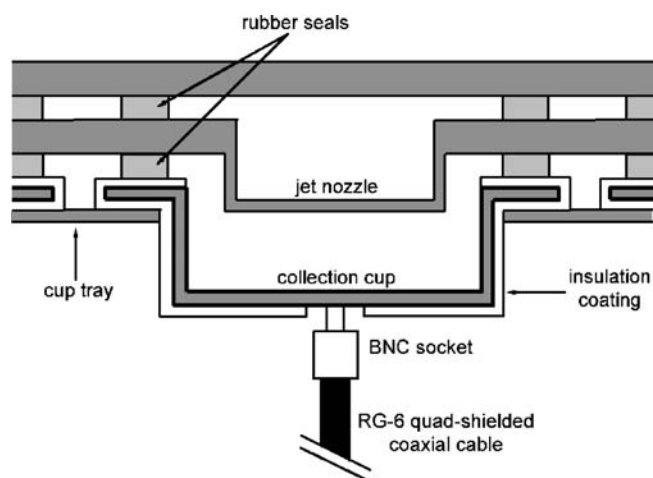


Fig. 2. Schematic diagram of an eNGI impaction stage.

Table I. Mean Current Measured by the eNGI, Where a Known Current Was Directly Applied to each Stage ($n=5$)

eNGI stage	Applied current											
	20 pA		50 pA		100 pA		200 pA		500 pA		1,000 pA	
	Mean	SD	Mean	SD	Mean	SD	Mean	SD	Mean	SD	Mean	SD
1	20.66	2.74	50.86	2.69	100.50	1.67	199.98	3.93	499.80	2.59	1,004.60	23.52
2	20.52	2.77	50.42	3.04	100.54	1.86	199.94	2.98	500.32	2.12	1,002.40	44.35
3	20.18	3.37	50.33	3.67	100.95	2.78	200.40	4.18	500.85	0.60	1,002.35	26.21
4	19.90	3.08	49.30	3.28	100.66	2.64	199.86	3.97	500.08	0.63	1,004.20	25.99
5	20.24	3.11	49.24	3.70	100.68	2.43	200.58	3.58	500.16	0.79	1,005.20	11.56
6	20.14	3.08	48.78	3.46	100.62	2.73	200.62	4.81	499.80	1.92	1,003.40	11.82
7	19.98	3.19	49.46	3.59	100.44	2.63	199.92	5.32	499.70	3.03	1,004.60	11.46
MOC	19.74	3.16	49.68	4.23	100.66	2.98	199.10	4.18	499.66	3.37	1,000.20	30.13

MATERIALS AND METHOD

eNGI Design

Like the ELPI, the eNGI is also essentially a series of Faraday wells, with an NGI enclosed within an earthed steel cage which acts as the outer conducting layer. The USP throat and NGI body are electrically isolated from each other by polypropylene adaptors (Fig. 1). The inner surface of the collection cups behave as the inner conducting layer, while the outer surface is covered with an acrylic latex coating, to ensure electrical isolation between cups, and from the NGI body (Fig. 2).

This coating is continuous with the exception of a small circular area, 15 mm in diameter, located at the centre of the cup base. A BNC socket (gold plated nickel terminal) acts as a metal probe which maintains electrical contact with the inner conducting layer via this exposed region. Each probe is connected through RG-6 quad-shielded coaxial cable to a Keithley 6517A electrometer (with K521 10-channel scanner card; Keithley Instruments, USA) (Fig. 1). In turn the electrometer is connected to a PC via RS-232 serial communication for data processing. This enables the real-time measurement of current within each of the stages (Fig. 2).

To confirm the capability of accurate current measurement by the eNGI setup, a series of 1 gigaohm resistors were connected to a DC power supply to generate known currents in the range of 20 pA to 1,000 pA, which were subsequently applied to each eNGI stage for 5 s at a scan speed of 1 scan/s. The mean measured currents, reported in Table I, were shown to be very close to the applied currents.

Metered Dose Inhalers

Three commercial products were chosen as model pMDIs for the investigation—Flixotide® (fluticasone propionate 250 µg/dose; Allen & Hanburys, Australia), Ventolin® (salbutamol sulfate 100 µg/dose; Allen & Hanburys, Australia) and QVAR® (beclomethasone dipropionate 100 µg/dose; iNova Pharmaceuticals, Australia). Each inhaler was primed once to waste as per manufacturer’s instructions. Following priming, five discrete actuations were each performed directly into the ELPI, NGI and eNGI. Charge and mass profiles were ascertained for each actuation.

Electrical Low-Pressure Impactor (ELPI)

Prior to each of five measurements, the 13 ELPI (Dekati, Finland) impaction stages were coated with silicon oil (Dow Corning, Australia) to minimize particle bounce. The corona charger was removed, as removal has not been found to affect ELPI performance (13). The electrometer range was set at 400,000 fA, and the baseline was zeroed. The inhaler was attached to the USP throat via a PTFE mouthpiece adaptor, a single dose was actuated into the ELPI and tested for 10 s at a flow rate of 30 l/min, while ELPIVI 4.0 software recorded current vs. time data for stages 1 to 12. Afterwards, the USP throat, corona charger frame, and each of the impaction stages were rinsed with either 5 ml 80:20 v/v methanol:water solution (Flixotide®), 5 ml deionised water (Ventolin®), or

Table II. Aerodynamic Cut-off Diameter Values for ELPI Stages 1–13, and NGI and eNGI Stages 1–7, at a Flow Rate of 30 l/min

Impaction stage	Aerodynamic cut-off diameter (µm)
ELPI	
13	9.98
12	6.61
11	4.01
10	2.4
9	1.6
8	0.951
7	0.615
6	0.383
5	0.263
4	0.157
3	0.0954
2	0.0574
1	0.0287
NGI and eNGI	
1	11.72
2	6.4
3	3.99
4	2.3
5	1.35
6	0.83
7	0.54

Table III. HPLC Setups for the Active Substances Salbutamol Sulfate (Ventolin[®]), Beclomethasone Dipropionate (QVAR[®]), and Fluticasone Propionate (Flixotide[®])

Active substance	Mobile phase (per 1 l)	Flow rate (ml/min)	Column	Injection volume (μ l)	UV absorbance wavelength (nm)
Salbutamol sulfate	600 ml methanol 400 ml deionised water 1 g sodium dodecyl sulfate	1.5	3.9 \times 150 mm Waters Nova-Pak [®] C ₁₈ column	100	276
Beclomethasone dipropionate	700 ml methanol 300 ml deionised water	1.0	3.9 \times 150 mm Waters Nova-Pak [®] C ₁₈ column	100	254
Fluticasone propionate	500 ml methanol 380 ml deionised water 100 ml acetonitrile 20 ml acetic acid	1.0	3.9 \times 150 mm Waters Nova-Pak [®] C ₁₈ column	50	242

5 ml 70:30 v/v methanol:water solution (QVAR[®]) into appropriate volumetric flasks, taken to volume and assayed with high-performance liquid chromatography (HPLC). The area under the curve was calculated for a current vs. time plot recorded for each impaction stage, giving a net charge value for that stage. Aerodynamic cut-off diameter values for ELPI stages at 30 l/min are shown in Table II.

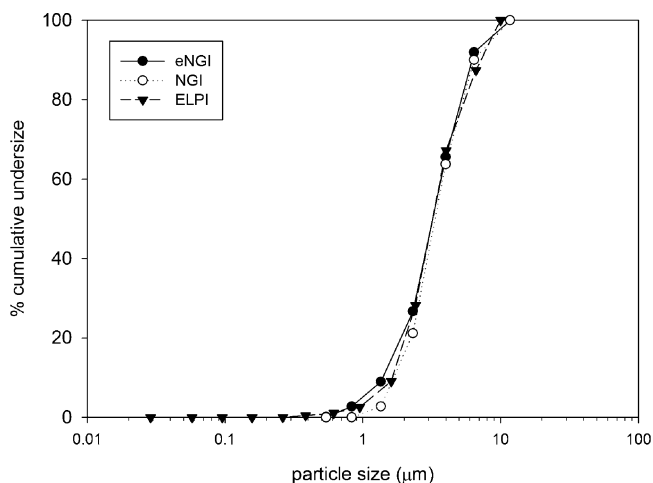
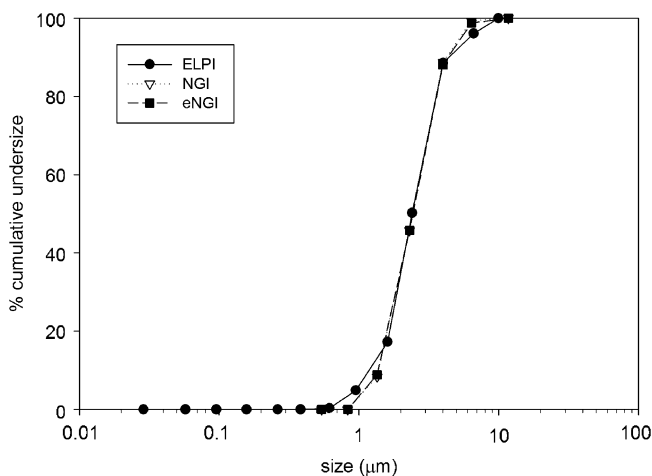
Next-Generation Impactor (NGI)

Before each NGI analysis, each of the collection cups were coated with silicon oil. The inhaler was connected to the USP throat using a PTFE mouthpiece adaptor, and a dose was actuated into the NGI (Copley Scientific, UK) at a vacuum flow rate of 30 l/min. The USP throat and collection cups were then each rinsed with either 5 ml 80:20 v/v methanol:water (Flixotide[®]), 5 ml deionised water (Ventolin[®]), or 5 ml 70:30 v/v methanol to water solution (QVAR[®]) into appropriate volumetric flasks, taken to volume and assayed by HPLC. Aerodynamic cut-off diameter values for NGI stages at 30 l/min are shown in Table II.

Electrical Next-Generation Impactor (eNGI)

As with the NGI, each of the collection stages were coated with silicon oil before each measurement. The electrometer range was set to 2 nA, and its scan speed was set to 10 channels/s. Before each run, the vacuum pump was switched on, while the electrometer was zeroed and given 30 s for baseline to settle. The inhaler was connected to the USP throat with a PTFE mouthpiece adaptor, and a dose was actuated into the eNGI at an air flow rate of 30 l/min for 10 s. The current vs. time data for each collection stage was acquired by the electrometer and recorded with Microsoft[®] Hyperterminal[™] (Microsoft Corporation, USA). The USP throat and collection cups were then each rinsed with either 5 ml 80:20 v/v methanol:water (Flixotide[®]), 5 ml deionised water (Ventolin[®]), or 5 ml 70:30 v/v methanol to water solution (QVAR[®]) into appropriate volumetric flasks, taken to volume and assayed by HPLC. The current vs. time plots recorded for each stage were integrated to give a net charge value for that stage.

Aerodynamic cut-off diameter values for NGI stages at 30 l/min were provisionally applied to eNGI data analysis.

**Fig. 3.** Cumulative undersize plots for Flixotide[®] in the ELPI, NGI and eNGI ($n=5$).**Fig. 4.** Cumulative undersize plots for Ventolin[®] in the ELPI, NGI and eNGI ($n=5$).

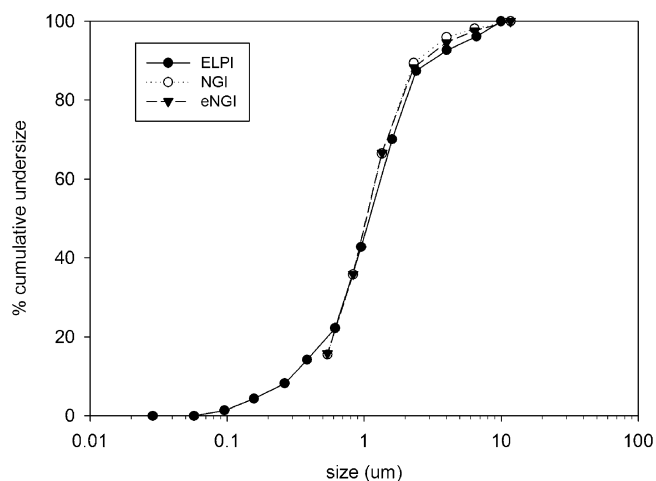


Fig. 5. Cumulative undersize plots for QVAR[®] in the ELPI, NGI and eNGI ($n=5$).

Any statistically significant differences observed between NGI and eNGI *in vitro* deposition and charge data for a particular pMDI formulation would suggest that the physical modifications in eNGI design have affected cut-off diameters.

HPLC Quantitative Analysis

Chemical analyses were performed using a Waters 600 model HPLC Controller, 2487 model dual-wavelength absorbance detector, 3.9×150 mm Waters Nova-Pak[®] C₁₈ column, and 515 model pump equipped with a 717plus model Autosampler. Data were recorded and integrated using Millennium Chromatography Software (Waters Corporation, Australia). HPLC setups for salbutamol sulfate, beclomethasone dipropionate, and fluticasone propionate are detailed in Table III.

Blister doses from a Flixotide[®] Accuhaler were emptied into a volumetric flask. The powder was dispersed in water to dissolve the lactose in the formulation. The resulting mixture was filtered using a vacuum filtration unit (Alltech, Australia), and the fluticasone propionate powder was recovered by drying the filter paper residue in a vacuum oven. Stock solution of fluticasone propionate was prepared in mobile phase using the extracted fluticasone powder. Samples were sequentially diluted in the appropriate mobile phase to fit within the linearity region of the HPLC analysis. Quantitation was based on peak area, using a standard curve, which was prepared daily. Standard solutions for fluticasone propionate were prepared at concentrations of 200, 100, 50, 10, 1, and 0.1 µg/ml. Salbutamol sulfate standard was acquired from S & D Chemicals (Sydney, Australia), with which standard

Table V. MMAD and GSD values for Ventolin[®] in ELPI, NGI and eNGI ($n=5$, mean ± SD)

	ELPI	NGI	eNGI
MMAD (µm)	2.44±0.11	2.40±0.09	2.41±0.06
GSD	1.56±0.29	1.51±0.02	1.54±0.03

solutions were prepared at 100, 30, 10, 3 and 1 µg/ml concentrations. Beclomethasone dipropionate standard was acquired from Sigma Chemicals (Perth, Australia), from which standard solutions were prepared at 50, 20, 10 1 and 0.5 µg/ml concentrations.

RESULTS AND DISCUSSION

Particle Size Distributions

Cumulative size distributions for Flixotide[®], Ventolin[®] and QVAR[®] in the three impactors are depicted in Figs. 3, 4 and 5 respectively. For each product, ELPI, NGI and eNGI size profiles appear to be comparatively similar. From these profiles, mass median aerodynamic diameter (MMAD) and geometric standard deviation (GSD) values for every impactor were calculated for Flixotide[®] (Table IV), Ventolin[®] (Table V) and QVAR[®] (Table VI).

Statistical analyses of differences in MMAD and GSD between impactors were carried out using unpaired t-tests, where a p -value < 0.05 was considered statistically significant. All differences in Flixotide[®] MMAD between ELPI, NGI and eNGI were not found to be statistically significant. The difference in Flixotide[®] GSD between the NGI and eNGI was not statistically significant. However, there was a statistically significant difference in GSD between the ELPI and NGI ($p=0.0002$), and ELPI and eNGI ($p=0.0046$). All differences in Ventolin[®] MMAD and GSD between the three impactors were not statistically significant. For QVAR[®], the differences in MMAD between the ELPI and NGI, and between ELPI and eNGI, were statistically significant ($p=0.0001$). Furthermore, there was also a statistically significant difference in GSD for the ELPI and eNGI ($p=0.0154$). All other differences between impactors in QVAR[®] MMAD and GSD were not statistically significant.

The similarity in MMAD and GSD between the NGI and eNGI for all three pMDIs suggests that the modifications made to the collection cups in the eNGI have not significantly affected its particle sizing capability. In comparison, the ELPI size profile was occasionally shown not to be in agreement with the NGI or the eNGI. This may perhaps confirm why the ELPI is not a pharmacopoeia method for particle sizing of pharmaceutical aerosols.

Table IV. MMAD and GSD values for Flixotide[®] in ELPI, NGI and eNGI ($n=5$, mean ± SD)

	ELPI	NGI	eNGI
MMAD (µm)	3.58±0.27	3.54±0.09	3.34±0.18
GSD	1.96±0.05	1.70±0.07	1.74±0.11

Table VI. MMAD and GSD values for QVAR[®] in ELPI, NGI and eNGI ($n=5$, mean ± SD)

	ELPI	NGI	eNGI
MMAD (µm)	1.13±0.02	1.04±0.02	1.04±0.02
GSD	1.97±0.05	1.91±0.04	1.89±0.03

Charge distributions

At an airflow rate of 30 l/min, the lower six stages of the ELPI have aerodynamic cut-off diameters smaller than stage 7 of the eNGI (0.54 μm). The micro-orifice collector (MOC) is not designed as an impactor stage, and has only a nominal cut-off diameter of 0.3 μm at 30 l/min (23, 24). As a result, there is no guarantee that the net charge measured in the MOC is comparable to the combined net charge of ELPI stages 1–6. For this reason, MOC charge data is omitted from the eNGI charge profile.

The mean MOC net charge for Flixotide[®] was 0.324 ± 0.090 nC, while ELPI stage 6 recorded a mean net charge of 0.300 ± 0.038 nC, and combined ELPI stages 1 to 6 recorded 1.19 ± 0.44 nC. For Ventolin[®], MOC mean net charge (-0.077 ± 0.076 nC) is also closer to that of ELPI stage 6 (-0.071 ± 0.012 nC) than ELPI stages 1 to 6 combined (-0.272 ± 0.059 nC). In addition, QVAR[®] MOC mean net charge (0.037 ± 0.051 nC) is closer to ELPI stage 6 (0.048 ± 0.024 nC) than ELPI stages 1 to 6 (0.14 ± 0.029 nC). This suggests that the MOC may behave more like ELPI stage 6, while the rest of the charge (equivalent to net charge in ELPI stages 1–5) is lost through the vacuum pump. It is understandable that this should be the case, given that the nominal cut-off diameter for MOC (0.3 μm) is somewhat comparable to ELPI stage 6 (0.383 μm).

There is good similarity in charge profiles between the ELPI and NGI for all three pMDIs, indicating that the design of the eNGI is capable of measuring net charge at a level comparable to the ELPI. Mean charge profiles for Flixotide[®] in the ELPI and eNGI are shown in Fig. 6. The two profiles overlap between 0.54 and 6.61 μm , where $86.4 \pm 1.6\%$ of the impacted dose (total amount of drug collected from all stages) is collected in the ELPI, and $87.5 \pm 3.7\%$ is collected in the eNGI. Mean charge profiles for Ventolin[®] in the ELPI and eNGI are shown in Fig. 7, which also overlap fairly well between 0.54 and 6.61 μm , where $91.6 \pm 1.8\%$ of the impacted dose is collected in the ELPI, and $96.0 \pm 2.0\%$ is collected in the eNGI. Mean charge profiles for QVAR[®] (Fig. 8) overlap well between 0.615 and 11.72 μm , where $78.8 \pm 0.8\%$ of the impacted dose is collected in the ELPI, and $65.3 \pm 1.3\%$ is collected in the eNGI.

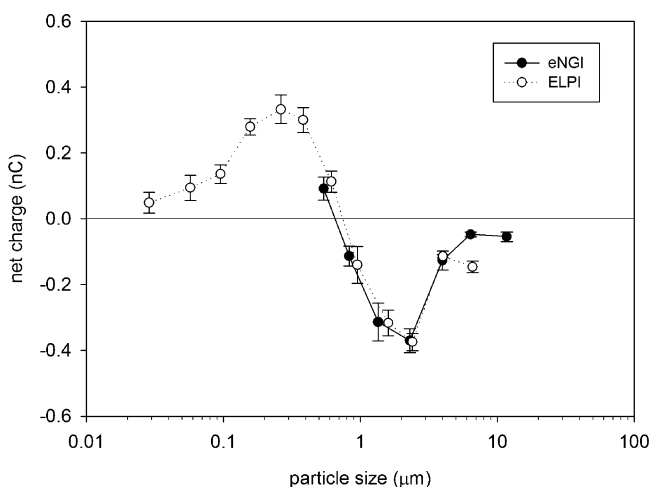


Fig. 6. Charge distributions for Flixotide[®] in ELPI and eNGI ($n=5$, mean \pm SD).

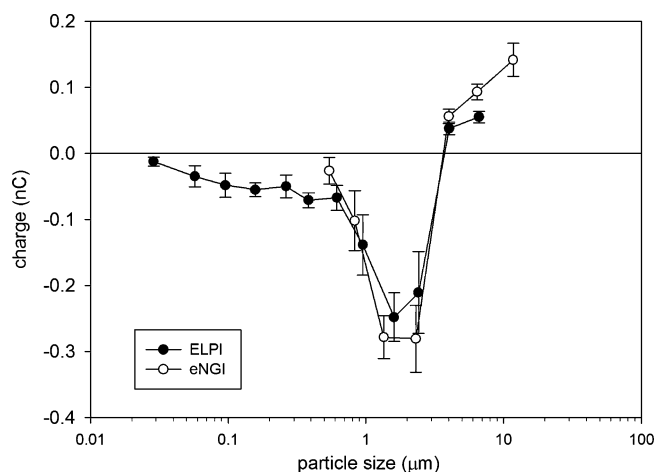


Fig. 7. Charge distributions for Ventolin[®] in ELPI and eNGI ($n=5$, mean \pm SD).

There is a noticeable difference in net charge between ELPI stage 12 (>6.61 μm) and eNGI stage 2 (>6.4 μm) for Flixotide[®] and Ventolin[®]. QVAR[®] was an exception, where the difference in net charge was not statistically significant. A possible explanation may lie in the fundamental difference in impactor layout upstream from these stages. ELPI stage 12 collects a smaller size fraction (6.61–9.98 μm) compared to eNGI stage 2 (6.4 μm –11.72 μm). However, the inbuilt ELPI electrometer is not connected to ELPI stage 13 (>9.98 μm), so net charge data cannot be obtained for this fraction. As a consequence, it is unknown whether the net charge measured from eNGI stage 2 may in fact be more similar to the net charge of ELPI stages 12 and 13 combined.

CONCLUSION

The eNGI has been shown in this study to be capable of measuring particle size distribution of a commercial pMDI product in a manner comparable to the NGI, a pharmacopoeia method. The investigators have also shown how the novel eNGI is capable of measuring charge profiles for commercial pMDIs at a similar capacity to the ELPI. The

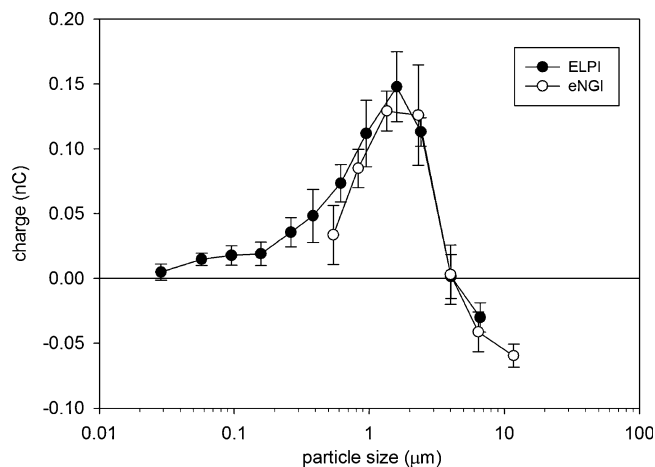


Fig. 8. Charge distributions for QVAR[®] in ELPI and eNGI ($n=5$, mean \pm SD).

eNGI has the potential to become a prototype for the design of a pharmacopoeic method for electrostatic characterization of inhalational formulations, including pMDIs, DPIs and nebulizers. Further studies are underway to assess the eNGI capability for DPIs.

ACKNOWLEDGMENTS

The authors would like to acknowledge Michael Pateron, Terry Pfeiffer and Herbert Chiou for their technical advice and expertise in assisting the construction of the eNGI, and Philip Kwok for his advice on the ELPI.

REFERENCES

1. P. C. L. Kwok, and H.-K. Chan. Electrostatic charge in pharmaceutical systems. In J. Swarbrick (ed.), *Encyclopedia of Pharmaceutical Technology*, Taylor & Francis, London, 2005, pp. 1–14.
2. M. García-Hernández, P. S. Bagus, and F. Illas. A new analysis of image charge theory. *Surf. Sci.* **409**:69–80 (1998). doi:10.1016/S0039-6028(98)00204-0.
3. C. Melandri, G. Tarroni, V. Prodi, T. de Zaiacomo, M. Formignani, and C. C. Lombardi. Deposition of charged particles in the human airways. *J. Aerosol. Sci.* **14**:657–669 (1983). doi:10.1016/0021-8502(83)90070-8.
4. A. G. Bailey, A. H. Hashish, and T. J. Williams. Drug delivery by inhalation of charged particles. *J. Electrostat.* **44**:3–10 (1998). doi:10.1016/S0304-3886(98)00017-5.
5. W. Balachandran, W. Machowski, E. Gaura, and C. Hudson. Control of drug aerosol in human airways using electrostatic forces. *J. Electrostat.* **40** & **41**:579–584 (1997).
6. D. Koolpiruck, S. Prakoonwit, and W. Balachandran. Numerical modelling of inhaled charged aerosol deposition in human airways. *IEEE Trans. Ind. Appl.* **40**:1239–1247 (2004). doi:10.1109/TIA.2004.834032.
7. D. Saini, J. Gunamgari, C. Zulaloglou, R. A. Sims, and M. K. Mazumder. Effect of electrostatic charge and size distributions on respirable aerosol deposition in lung model. In I. I. A. Society (ed.), *39th Annual IAS Meeting (IEEE Industry Applications Society)*, Vol. 2, IEEE, Seattle, 2004.
8. A. G. Bailey. Charging of solids and powders. *J. Electrostat.* **30**:167–180 (1993). doi:10.1016/0304-3886(93)90072-F.
9. M. D. Hogue, C. R. Buhler, C. I. Calle, T. Matsuyama, W. Luo, and E. E. Groop. Insulator–insulator contact charging and its relationship to contact pressure. *J. Electrostat.* **61**:259–268 (2004). doi:10.1016/j.elstat.2004.03.002.
10. M. Murtooma, P. Harjunen, V. Mellin, V. Lehto, and E. Laine. Effect of amorphicity on the triboelectrification of lactose powder. *J. Electrostat.* **56**:103–110 (2002). doi:10.1016/S0304-3886(02)00066-9.
11. D. J. Lacks, and A. Levandovsky. Effect of particle size distribution on the polarity of triboelectric charging in granular insulator systems. *J. Electrostat.* **65**:107–112 (2007). doi:10.1016/j.elstat.2006.07.010.
12. A. G. Bailey. The charging of insulator surfaces. *J. Electrostat.* **51–52**:82–90 (2001). doi:10.1016/S0304-3886(01)00106-1.
13. W. Glover, and H. K. Chan. Electrostatic charge characterization of pharmaceutical aerosols using electrical low-pressure impactor (ELPI). *J. Aerosol. Sci.* **35**:755–764 (2004). doi:10.1016/j.jaerosci.2003.12.003.
14. P. C. L. Kwok, W. Glover, and H. K. Chan. Electrostatic charge characteristics of aerosols produced from metered dose inhalers. *J. Pharm. Sci.* **94**:2789–2799 (2005). doi:10.1002/jps.20395.
15. P. M. Young, A. Sung, D. Traini, P. Kwok, H. Chiou, and H. K. Chan. Influence of humidity on the electrostatic charge and aerosol performance of dry powder inhalers carrier-based systems. *Pharm. Res.* **24**:963–970 (2007). doi:10.1007/s11095-006-9218-8.
16. A. G. Bailey. The inhalation and deposition of charged particles within the human lung. *J. Electrostat.* **42**:25–32 (1997). doi:10.1016/S0304-3886(97)00134-4.
17. P. R. Byron, J. Peart, and J. Staniforth. Aerosol electrostatics I: Properties of fine powders before and after aerosolisation by dry powder inhalers. *Pharm. Res.* **14**:698–705 (1997). doi:10.1023/A:1012181818244.
18. M. Murtooma, P. Pekkala, T. Kalliohaka, and J. Paasi. A device for aerosol measurement and sampling. *J. Electrostat.* **63**:571–575 (2005). doi:10.1016/j.elstat.2005.03.018.
19. M. Dawson, P. Burnell, W. Balachandran, J. Kulon, and S. Sivathasan. A novel bipolar charge measurement system for characterizing aerosols, *Respiratory Drug Delivery VIII*, Tucson, AZ, USA, 2002, pp. 443–445.
20. J. Keskinen, K. Pietarinen, and M. Lehtimäki. Electrical low pressure impactor. *J. Aerosol. Sci.* **23**:353–360 (1992). doi:10.1016/0021-8502(92)90004-F.
21. J. C. Orban, and J. Peart. Simultaneous electrostatic charge characterization and particle size analysis of metered dose inhalers (pMDIs) using the electrical low pressure impactor. *Respiratory Drug Delivery IX*, 2004.
22. M. Marjamäki, J. Keskinen, D. R. Chen, and D. Y. H. Pui. Performance evaluation of the electrical low-pressure impactor. *J. Aerosol. Sci.* **31**:249–261 (2000). doi:10.1016/S0021-8502(99)00052-X.
23. V. A. Marple, D. L. Roberts, F. J. Romay, N. C. Miller, K. G. Truman, M. van Oort, B. Olsson, M. J. Holroyd, J. P. Mitchell, and D. Hochrainer. Next generation pharmaceutical impactor (a new impactor for pharmaceutical inhaler testing). Part I: Design. *J. Aerosol. Med.* **16**:283–299 (2003). doi:10.1089/089426803769017659.
24. C. Dunbar, and J. Mitchell. Analysis of cascade impactor mass distributions. *J. Aerosol. Med.* **18**:439–451 (2005). doi:10.1089/jam.2005.18.439.